Self-Oscillating Fluxgate Current Sensor with Pulse Width Modulated Feedback

Radivoje Đurić and Milan Ponjavić

***Abstract*—A self-oscillating fluxgate current sensor with pulse-width modulated feedback is discussed in the paper. The current feedback creates additional dissipation in the circuit which could be reduced by applying the method of pulse-width modulation. For simplicity, the pulse-width modulator is realized as a self-oscillating structure whose frequency is adjusted by means of the hysteresis of a regenerative comparator, and the feedback is realized with no additional winding.**

***Index Terms*—Fluxgate, self-oscillating, pulse-width modulation.**

I. Introduction

THE most widespread sensors for galvanically insulated measurement of current are, at present, sensors based on the Hall-effect. The cheap open-loop Hall-effect sensors having low consumption, and of relatively low accuracy are realized as a silicon chip set in the air gap of a ferrite core [1]. The closed-loop Hall sensors having feedback have better metrological characteristics, linearity, accuracy, and bandwidth, but also a considerably higher consumption owing to the current which compensates the action of the measured current in the ferrite core. Both types have high values of the voltage offsets and drifts**.**

The fluxgate current sensors have the best metrological characteristics and have a considerably better sensitivity compared to the Hall-effect sensors. A standard realization of these sensors is carried out by the two windings, excitation and measuring, which are wound on a toroid magnetic core [2]. Through the excitation winding flows variable current causing a periodic saturation of the core. The conductor carrying the measured current passes through the center of the toroid and creates the asymmetry in the magnetic field of the core, which causes its asymmetric saturation, i.e. the appearance of even harmonics. The most frequently applied are the sensors detecting the second harmonic and a high linearity is accomplished by closing the feedback loop. When realized with the cores having no air gaps, they are, compared to the Hall effect sensors, insensitive to the influences of external magnetic fields. The commercial versions of thesesensors have one order of magnitude better characteristics compared to the sensors based on the Hall-effect, but they are considerably more expensive.

There is a room for a class of sensors which have better immunity to external electromagnetic fields and better temperature variation of the characteristics compared to the sensors based on the Hall element, and which have good characteristics of the fluxgate current sensors, but are considerably simpler for realization, the so called self-oscillating fluxgate current sensors.

R. Đurić (e-mail: radivoje@gmail.com) and M. Ponjavac (e-mail: milan@el.etf.rs) are with the Faculty of Electrical Engineering, University of Belgrade, Serbia.

II. Self-Osillating Fluxgate Current Sensor

Compared to the classic fluxgate current sensor, the self-oscillating sensor operates based on the principle of autonomous generation of excitation for the secondary of the current transformer which serves for obtaining information on the current of the primary. This is voltage excitation and the self-oscillation process limits the excitation current of the secondary winding.

Fig. 1a shows an open-loop self-oscillating fluxgate current sensor. The basis of this sensor is the core whose simplified nonlinear characteristic is shown in Fig. 1b, where: L_m and L_{sat} are the magnetization inductances of the secondary when the core is not saturated and saturated, respectively, I_{sat} and φ_{sat} are the current and magnetic flux bringing the core to saturation. Thresholds of the Schmitt comparator are symmetric $V_{TL} = -V_{TH}$, therefore the corresponding current thresholds $I_{SL} = -I_{SH} = -V_{TH}/R_S$ are also symmetric. On the core characteristic of Fig. 1b the times, from t_1 to t_7, which correspond to the movement of the oscillator operating point during one full period at steady state are marked. Since $L_m >> L_{sat}$, time intervals when the core is saturated, $t_2 - t_4$ and $t_5 - t_7$ are much shorter compared to the interval when the core is not saturated, thus the period of the self-oscillating process is approximately equal to

$$T_S \approx \Delta t_1 + \Delta t_2 , \tag{1}$$

where $\Delta t_1 = t_2 - t_1$ and $\Delta t_2 = t_5 - t_4$.

At the initial moment of observation, $t = t_1$, the core comes out of negative saturation, thus

$$i_S(t) = i_S(\infty) + \left(i_S(t_1^+) - i_S(\infty)\right) e^{-\frac{t-t_1}{\tau}} , \; t_1 \le t \le t_2 , \tag{2}$$

where the time constant is $\tau = L_m/R_S$.

Since inductance L_m is large, $\tau >> \Delta t_1$, Δt_2, i.e. $e^{-t/\tau} \approx 1 - (t/\tau)$, and expression (2) can be simplified:

$$i_S(t) = i_S(t_1^+) + \left(i_S(\infty) - i_S(t_1^+)\right)\frac{t-t_1}{\tau},\ t_1 \le t \le t_2, \quad (3)$$

$$i_S(t_1^+) = (I/n) - I_{sat} = I_{EQ} - I_{sat} \quad (4)$$

$$i_S(\infty) = V_{DD}/R_S, \quad (5)$$

where I_{EQ} is the equivalent measured secondary current.

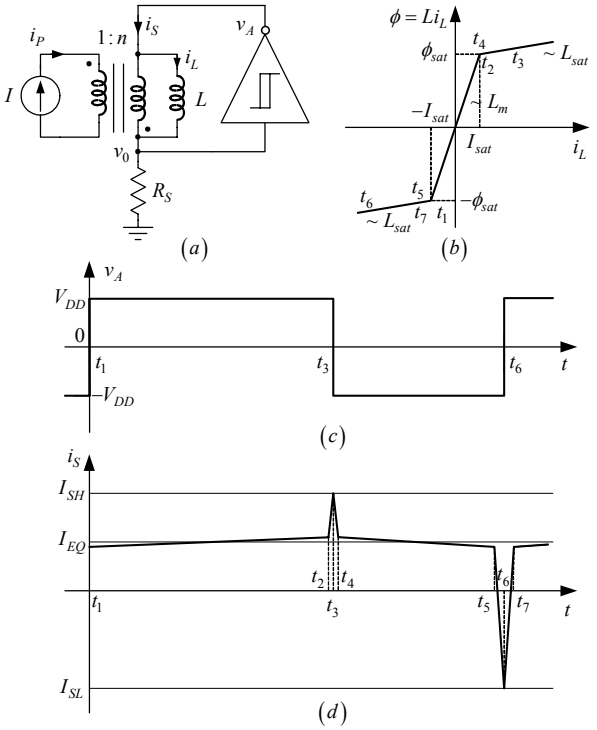

Fig. 1. The characteristic diagram of the open-loop self-oscillating fluxgate current sensor.

At the end of time interval Δt_1 the core is at the threshold of the positive saturation, i_L=I$_{sat}$, thus $i_S(\Delta t_1)$= I_{EQ} + I_{sat}, wherefrom one obtains

$$\Delta t_1 = \frac{2L_m I_{sat}}{V_{DD} - R_S I_{EQ} + R_S I_{sat}}. \quad (6)$$

In a similar way time interval Δt_2 is:

$$\Delta t_2 = \frac{2L_m I_{sat}}{V_{DD} + R_S I_{EQ} + R_S I_{sat}} \quad (7)$$

From (6) and (7), the approximate value of the period of oscillations is

$$T_S \approx \Delta t_1 + \Delta t_2 \approx \frac{4L_m I_{sat} V_{DD}}{V_{DD}^2 - \left(R_S I_{EQ}\right)^2},\ I_{EQ} \gg I_{sat}. \quad (8)$$

Since the average value of voltage across the coil is equal to zero, the average value of the output voltage is

$$\overline{v}_0 \approx V_{DD}\frac{\Delta t_1 - \Delta t_2}{\Delta t_1 + \Delta t_2} \approx R_S I_{EQ},\ V_{DD} \gg R_S I_{sat}. \quad (9)$$

When the time interval of core in saturation is negligibly small compared to the interval when the core is not in saturation, the average value of current i_S is equal to the equivalent secondary current I_{EQ}. Then the slope of the linearized transfer characteristic

$$\overline{i}_0 = \overline{v}_0 / R_0 = f\left(I_{EQ}\right) \quad (10)$$

is equal to one. Duration of the time interval when the core is saturated is finite and changes as a function of the measured current, thus in practice the slope of the transfer function is always less than one. Influence of the hysteresis losses in the ferrite core is significant only when the hysteresis loop has large coercive field and magnetic field in saturation B_{sat}. When parameter variation of the ferrite core and control electronics is small, fluxgate current sensors without feedback are an adequate solution in applications where a cheap sensor and accuracy not better than 0.5% are required [3].

III. Closed-Loop Self-Oscillating Fluxgate Current Sensor

Static gain of the open-loop self-oscillating current sensor and maximum error of linearity, both dependent on sensor parameters and environmental conditions, are most sensitive to supply voltage variations. Closing the feedback loop is used in applications where the precise measurement of current, a wide bandwidth, and small variations of the gain and linearity with parameter variations are required. It can be realized according to the simplified scheme shown in Fig. 2, [4].

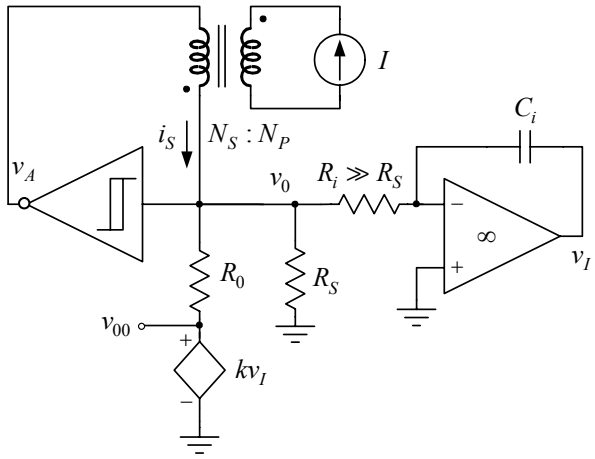

Fig. 2. Closed-loop self-oscillating fluxgate current sensor.

According to Fig. 2

$$V_I(s) = -\frac{1}{sT_i}V_0(s),\ T_i = \frac{1}{C_i R_i}, \quad (11)$$

$$I_s(s) = \frac{V_0(s)}{R_S \parallel R_0} - \frac{V_{00}(s)}{R_0},\ V_{00}(s) = kV_i(s), \quad (12)$$

giving,

$$\frac{V_{00}(s)}{I_s(s)} = -\frac{R_0}{1 + \frac{sT_i}{k}\left(1 + \frac{R_0}{R_S}\right)} \quad (13)$$

and

$$Y_{0S}(s) = \frac{I_s(s)}{V_0(s)} = \left(\frac{1}{R_S} + \frac{1}{R_0}\right) + \frac{k}{sT_i R_0}. \quad (14)$$

On the basis of Fig. 2 and expression (14) it follows:

$$V_a(s) - V_I(s) = V_0(s) \text{ and } I_s(s) = Y_{0S}(s)V_0(s), \quad (15)$$

where from a block diagram is obtained which represents the circuit for regulation of current i_S, Fig. 3.

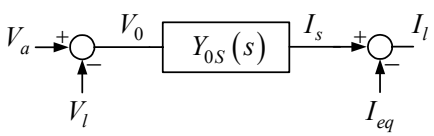

Fig. 3. Block diagram of the circuit for regulation of current i_S.

Since transfer function $Y_{0S}(s)$ is of the form of a PI regulator,

$$PI(s) = G_1 + \frac{G_2}{s},\ G_1 = \frac{1}{R_S} + \frac{1}{R_0},\ G_2 = \frac{k}{T_i R_0}, \qquad (16)$$

it is concluded that the steady state error reduces towards zero, i.e.

$$V_0(0) \to 0,\ I_l(0) \to 0,\ I_s(0) \to I_{eq}. \qquad (17)$$

Ideally, by means of an integrator and a controlled voltage source kv_1, $k>0$, it can be ensured that the average value of v_0 is equal to zero. This means that the variable and DC components of current i_S close their loops through resistors R_S and R_0, respectively, giving at the output the equivalent value of the DC measured current

$$v_{00} = -R_0 \bar{i}_S = -R_0 I_{EQ} = -R_0 I / n. \qquad (18)$$

Owing to a strong feedback, positive and negative peaks of the secondary current are of the same absolute value, thus the static gain is equal to one. Since the stray inductances are connected in series with the secondary winding, they do not affect the error of the static gain at steady state.

When the feedback loop is closed, an average current I_{EQ} is established through this contour and since there are significant voltage drops, the power dissipated in the circuit is increased. When the controlled voltage generator kv_I, or integrator output for k=1, are realized so that the output stages are in class A, B, or AB, they dissipate relatively high power, the consumption is increased and this may cause drifts of the current sensor characteristic, static gain, and linearity.

IV. Pulse-Width Modulation Feedback

In order to reduce dissipation in the circuit of the current sensor a pulse-width modulator and a class D amplifier are used. Output stage of the class D amplifier contains switching transistors which ideally dissipate zero power, owing to zero current when turned off or zero voltage when turned on.

There are several types of pulse-width modulators, and they can be divided in two large groups. The first group consists of modulators having external generator of «triangular carrier», while modulators of the second group generate internally the carrier frequency, the so called self-oscillating pulse-width modulators [5]. Because of its simplicity the self-oscillating pulse-width modulator, shown in simplified form in Fig. 5., has been selected to close the feedback loop.

In the absence of the driving signal, v_I = 0, the circuit oscillates at a frequency which corresponds to the modulus of the loop gain equal to one and zero phase. Since the feedback is returned to the negative input terminal, the self-oscillation requires an additional phase shift of 180° at the carrier frequency. This is provided by an integrator which introduces 90° phase shift and a phase delay through the comparator circuit and output switching transistors which add additional 90°. The comparator could be with or without hysteresis, depending on the desired carrier frequency. If there is no hysteresis, the frequency is determined by the delay introduced by the comparator circuit, while introduction of a hysteresis results in adjustment of the carrier frequency by the width of the hysteresis loop [6]

$$f_{PWM} = \frac{1 - M^2}{4(V_H / V_{DD}) T_{iPWM}}, \qquad (19)$$

where: V_H – width of the hysteresis loop, T_{iPWM} – time constant of the integrator, and M – modulation index of the pulse-width modulator.

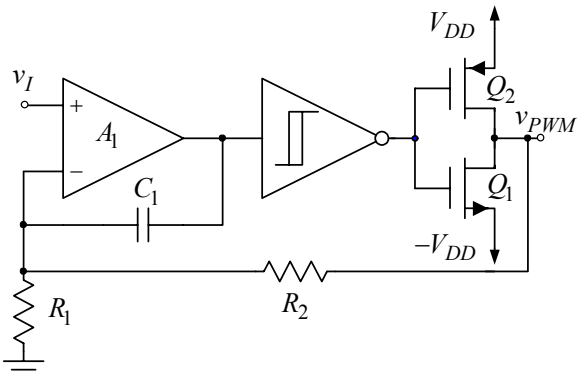

Fig. 4. Self-oscillating pulse-width modulator.

Low frequency signal is fed to input v_I of the amplifier and by the comparator and current feedback it is ensured that the output voltage of the modulator is pulse-width modulated and proportional to the input voltage. This voltage drives switches Q_1 and Q_2 and ensures low dissipation in them, i.e. efficient signal amplification.

The modulating frequency is much higher than the driving frequency, thus the transfer function of the modulator at the driving frequency

$$H_{PWM}(s) = \frac{V_{pwm}(s)}{V_i(s)} = \left(1 + \frac{R_2}{R_1}\right) \frac{1 + sC_1(R_1 \| R_2)}{1 + sC_1 R_2 / k_{PWM}}, \qquad (20)$$

where k_{PWM} is the gain from the output of amplifier A_1 up to output v_{PWM}.

Losses in the pulse-width modulator circuit can be presented in the form [7]

$$P_{PWM,loss} = P_{sw} + P_{cond} + P_g. \qquad (21)$$

In expression (21): P_{sw} – switching losses in the drain circuit,

$$P_{sw} = 0,5 C_{OSS} V_{DD}^2 f_{PWM} + I_{PWM} V_{DD} (t_f + t_r) f_{PWM}, \qquad (22)$$

where: $C_{OSS} = C_{ds} + C_{gd}$ are output capacitances of the switching transistors, $C_{OSS} = C_{OSS1} + C_{OSS2}$, t_r *and* t_f are the turn-on and turn-off times of the transistors, respectively; P_{cond} – conduction losses in the switching transistors,

$$P_{cond} = R_{on1,2} I_{PWM,rms}^2, \qquad (23)$$

where R_{on} are the switch resistances, $R_{on1,2} = R_{on1} + R_{on2}$ and $I_{PWM, rms}$ is the rms value of the output terminal current of the PWM modulator, and P_g - switching losses in the gate circuit,

$$P_g = Q_{g1,2} V_{DD} f_{PWM}, \quad (24)$$

where Q_g is the charge required by the gate in order to turn on the switching transistor, $Q_{g1,2} = Q_{g1} + Q_{g2}$.

V. Experimental Result

In Fig. 5. the prototype of the sensor of Fig. 2. with pulse-width modulated feedback is shown. By resistive divider R_1 / R_2 and battery supply $V_{DD} = 2{,}5\ \text{V}$ thresholds of the comparator are adjusted to values $V_{TH} = -V_{TL} = 0{,}1\ \text{V}$, while $R_S = R_0 = 1\,\Omega$, $C_F = 3{,}3\ \mu\text{F}$, $L_F = 47\ \mu\text{H}$, and $T_i = 10\ \text{ms}$. Comparator circuit *comp* is realized by using standard LM311 comparator and Schmitt circuits 74HC14 which serve for shaping of driving pulses for the switching transistors ZXM64N02 and ZXM64P02. Ferrite core R12.5 made of standard ferromagnetic material N30 and N_S = 200 turns is used in the prototype. Switching frequency of the pulse-width modulator, where the same switching transistors as in the circuit of the current sensor with no feedback are used, is adjusted to 150kHz.

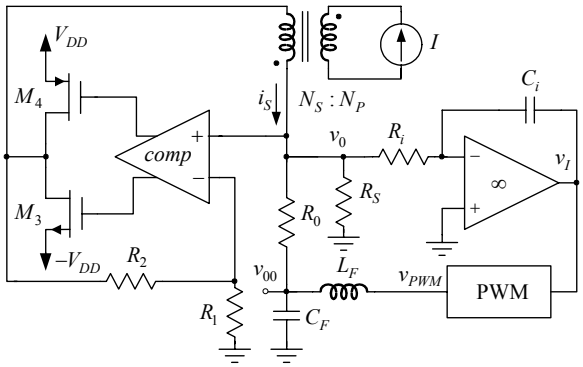

Fig. 5. Prototype of the self-oscillating current sensor with pulse-width modulated feedback.

By using prototype of Fig. 5 transfer characteristic of the current sensor $-\frac{N_S}{N_P}\frac{V_{00}}{R_0} = f(I)$, for the range of measured currents $-20\ \text{A} \le I \le 20\ \text{A}$, is taken and shown in Fig. 6.

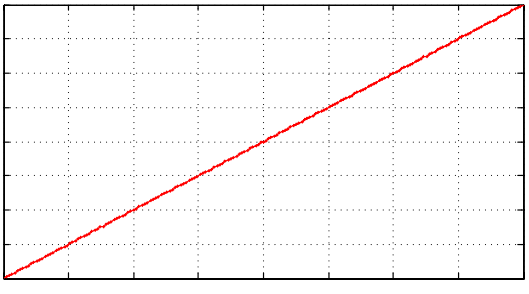

Fig. 6. Static transfer characteristic of the current sensor of Fig. 5.

Static gain of the current sensor $k_L = 0.999$ was obtained by curve fitting, while the maximum error of linearity was $\delta_{Lmax} = 0.1\%$.

Simultaneously, the record is made of the power consumption as function of the measured current, shown in Fig. 7, indicating that the maximum consumption of the current sensor amounted $P_{DD\max} \approx 70\ \text{mW}$. Dominant losses in the circuit are the conductive losses in resistances of the switches, coil, and resistance R_0, approximately amounting $P_{cond} \approx 40\text{mW}$. Switching losses in the drain circuit can be neglected, while $P_g \approx 5\text{mW}$. Owing to the self-oscillation, in the absence of the measured current somewhat less than 30mW is dissipated in the circuit. Variation of the switching frequency with variation of the consumption is small. Since low level currents are being switched, levels of the generated electromagnetic noise are low.

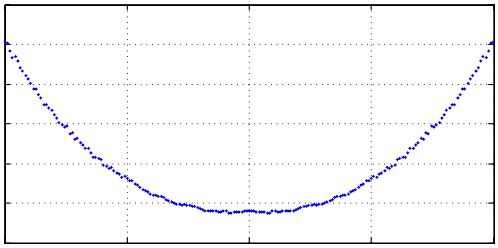

Fig. 7. Dependence of the power consumption as function of the measured current.

VI. Conclusion

On the basis of theoretical considerations a self-oscillating fluxgate current sensor with pulse-width modulated feedback has been realized. Fig. 6. indicates that this sensor has practically ideal transfer characteristic, which is a consequence of a strong negative feedback, while Fig. 7. shows that the current sensor has a very small consumption, 70mW at the most. Due to the good properties of negative feedback, the sensor is insensitive to variations of the supply voltage and circuit parameters. Due to pulse-width modulation is has low consumption, thus the sensor offers itself as a cheap and reliable solution for galvanically insulated measurement of DC current.

References

[1] P.Ripka, "Current sensors using magnetic materials", Journal of optoelectronics and advanced materials, vol. 6, no. 2, pp. 587-592, June 2004.

[2] F. Primdahl, "The fluxgate mechanism, Part 1", IEEE Transactions on Magnetics, vol. 6, pp. 376-383, 1970.

[3] R. Đurić, M. Ponjavić, N. Smiljanić, "Galvanically insulated current sensor having digital output", INFOTEH-Jahorina, Vol. 8, pp. 379-383, March 2009.(in Serbian)

[4] P. Pejović, "A simple circuit for direct current measurement using a transformer", IEEE Transactions Circuits and Systems, vol. 45, no. 8, pp. 830-837, August 1998.

[5] B. Putzeys, "Simple Self-Oscillating Class D Amplifier with Full Output Filter Control", 118th AES Convention, Barcelona, May 2005.

[6] M. Berkhout, L. Breems, E. Tuijl, "Audio at Low and High Power", ESSCIRC 2008, pp. 40-49, September 2008.

[7] J. Honda, J. Adams, "Class D Audio Amplifier Basics", International Rectifier Application Note AN-1071.